Combustion Theory and Modelling
Vol. 9, No. 2, May 2005, 365–383

Taylor & Francis
Taylor & Francis Group

Quantification of differential diffusion in nonpremixed systems

J. C. SUTHERLAND*†, P. J. SMITH‡, and J. H. CHEN§

†Sandia National Laboratories, Albuquerque, NM 87185, USA
‡Department of Chemical Engineering, University of Utah, Salt Lake City, UT 84112, USA
§Combustion Research Facility, Sandia National Laboratories, Livermore, CA 94551, USA

Most attempts to quantify differential diffusion (DD) are based on the difference between different definitions of the mixture fraction. This paper presents a general method for evaluating differential diffusion in premixed or nonpremixed systems based on conservation equations for the elemental mass fractions. These measures form a basis for analysing differential diffusion. Casting these in terms of a mixture fraction gives particular insight into differential diffusion for nonpremixed systems, and provides a single DD measure. Furthermore, it allows direct evaluation of the validity of the traditional assumptions involved in writing a mixture fraction transport equation. Results are presented for one-dimensional opposed flow simulations of hydrogen and methane flames as well as direct numerical simulations (DNS) of CH_4/H_2–air and CO/H_2–air flames. For a common definition of the mixture fraction, the DD measure can be approximated well by considering only the contribution of H_2 and CH_4 in methane–air flames. Differential diffusion is largely driven by production of H_2 in the flame zone for hydrocarbon flames. Effects of strain rate and filter width on the relative importance of differential diffusion are examined.

1. Introduction

Many nonpremixed combustion models rely on the assumption that the mixture fraction is a conserved scalar. Under that assumption, a mixture fraction transport equation is solved and a complex state relationship (such as equilibrium or laminar flamelet behaviour) is hypothesized to relate the thermochemical state of the system to the mixture fraction. A sufficient condition for the mixture fraction to be a conserved scalar is for all species to have equal mass diffusivity [1–4]. An inconsistency, however, arises when one wishes to incorporate differential diffusion (DD) effects into a state relationship because the equation governing the evolution of the mixture fraction itself is only valid under the assumption of negligible DD.

Alternatively, a more abstract definition of the mixture fraction as simply a 'conserved scalar' may be employed to relax the assumption of equal diffusivities and allow incorporation of DD effects [5]. This approach allows DD to be incorporated into the state relationship while maintaining consistency in the mixture fraction evolution equation. This approach, however, relies on the assumption that there exists a definition of the mixture fraction such that it is a

*Corresponding author. E-mail: jnsuthe@sandia.gov

Combustion Theory and Modelling
ISSN: 1364-7830 (print), 1741-3559 (online)
http://www.tandf.co.uk/journals
DOI: 10.1080/17455030500150009

conserved scalar. If no such definition exists, then this approach is not self-consistent. Recent theoretical work [4] suggests that there may exist a definition of the mixture fraction that is conserved in the presence of DD, but no such definition has yet emerged.

Thus, quantification of DD has important implications for modelling approaches as well as fundamental understanding of combustion processes. A priori knowledge of the importance of DD for a given combustion system may influence modelling approaches. This requires a method to obtain a quantitative measure of the amount of DD occurring. Most previous attempts at quantifying DD have fallen into one of two categories:

1. Computational studies of DD using simple models for diffusion in their analysis, applied to either nonreacting flows [6–8] or isothermal flows with one-step global chemistry [9]. Because of the simple transport and lack of detailed chemistry, the measures proposed for DD are not directly applicable in the case of multispecies reacting flow with detailed transport.
2. Experimental data [10, 11], one-dimensional laminar flame simulations [12], and one-dimensional turbulence (ODT) simulations [13] in which DD was measured by examining differences between elemental mixture fractions. This technique can generally be applied to reacting flows, but does not provide a full measure of DD. Furthermore, this approach provides only an indirect measure of the amount of DD occurring, i.e. differences between elemental mixture fractions indicate some amount of DD, but do not provide quantitative measures of DD.

This paper presents a new measure of DD based on the general evolution equations for the elemental mass fractions. This provides one measure of DD for each element in a reacting system, thereby forming a complete measure of DD. By introducing the concept of the mixture fraction, a single (non-unique) measure of DD is obtained. For a given definition of the mixture fraction, this approach provides direct quantification of DD as well as its effect on the mixture fraction evolution equation. One-dimensional simulations of methane–air and hydrogen–air opposed-jet flames as well as direct numerical simulations (DNS) of two-dimensional CH_4/H_2–air turbulent jets are used to demonstrate the utility of this approach. The significance of DD in methane flames is compared with the significance of hydrogen–air flames and the effect of strain rate on the importance of DD is investigated. The species contributions to the proposed measure of DD are examined to determine the feasibility of using the new measure experimentally. Finally, in the context of large eddy simulation (LES), the effect of the filter size on the relative importance of DD on the filter scale is examined.

2. Quantification of DD

Let us define a conserved scalar as a quantity whose evolution equation may be written in convection form as

$$\rho \frac{D\phi}{Dt} = \nabla \cdot (\rho D_\phi \nabla \phi), \tag{1}$$

where ρ is the mixture mass–density, D_ϕ is the effective diffusivity of ϕ, and $\frac{D}{Dt} \equiv \frac{\partial}{\partial t} + \mathbf{u} \cdot \nabla$ is the material derivative operator. In other words, we define a conserved scalar as one whose diffusive flux is directly proportional to its gradient and whose governing equation contains no source terms. For the purposes of this paper, we define differential diffusion as any deviation from the diffusive flux implied by equation (1), i.e. $\mathbf{j}_\phi = \rho D_\phi \nabla \phi$, where $\mathbf{j}_\phi$ is the mass-diffusive flux of ϕ relative to the mass-averaged system velocity, $\mathbf{u}$ (see Appendix for details).

The species evolution equations may be written in convection form as

$$\rho \frac{DY_i}{Dt} = -\nabla \cdot \mathbf{j}_i + W_i \dot{\omega}_i \tag{2}$$

where Y_i is the mass fraction of species i, $\mathbf{j}_i$ is the mass diffusion flux of species i relative to a mass-averaged velocity (see Appendix for details), W_i is the species molecular weight, and $\dot{\omega}_i$ is the net molar production rate of species i. The elemental mass fractions, Z_ℓ, may be written in terms of species mass fractions as

$$Z_\ell = \sum_{i=1}^{N_s} \frac{a_{\ell,i} W_\ell}{W_i} Y_i, \tag{3}$$

where N_s is the number of species, $a_{\ell,i}$ is the number of atoms of element ℓ in species i, W_ℓ is the molecular weight of element ℓ, and W_i is the molecular weight of species i. Unless explicitly stated otherwise, subscripts i and j will be used for species, while subscripts ℓ and m will be used to indicate elements. Using equations (2) and (3), conservation equations for the N_e elemental mass fractions are written as

$$\rho \frac{DZ_\ell}{Dt} = -\sum_{i=1}^{N_s} \frac{a_{\ell\, i} W_\ell}{W_i} \nabla \cdot \mathbf{j}_i. \tag{4}$$

In the limiting case where $\mathbf{j}_i = -\rho D \nabla Y_i$, (see Appendix for details, and also note the assumption $D_i = D_j = D$) then equation (4) may be written as

$$\rho \frac{DZ_\ell}{Dt} = \nabla \cdot (\rho D \nabla Z_\ell). \tag{5}$$

This implies that, under the assumption that the species diffusive fluxes may be written as $\mathbf{j}_i = -\rho D \nabla Y_i$, all elemental mass fractions are conserved scalars as defined by equation (1). Furthermore, as we shall see, this assumption also allows all elemental compositions to be related to a single quantity: the mixture fraction. The difference between equations (4) and (5) is caused by differential diffusion. Subtracting equation (5) from equation (4), we obtain

$$\rho \frac{DZ_\ell}{Dt} = \nabla \cdot (\rho D \nabla Z_\ell) + \varepsilon_\ell, \tag{6}$$

where ε_ℓ is defined as

$$\varepsilon_\ell \equiv \underbrace{-\sum_{i=1}^{N_s} \frac{a_{\ell\, i} W_\ell}{W_i} \nabla \cdot \mathbf{j}_i}_{\Upsilon_\ell^{\text{exact}}} - \underbrace{\nabla \cdot (\rho D \nabla Z_\ell)}_{\Upsilon_\ell^{\text{approx}}}. \tag{7}$$

The terms $\Upsilon_\ell^{\text{exact}}$ and $\Upsilon_\ell^{\text{approx}}$ in equation (7) identify the exact and approximate diffusion terms, respectively, and will be used throughout the remainder of the document.

Equation (6) represents an exact transport equation for the elemental mass fractions, without any assumptions involving diffusive fluxes. The effects of differential diffusion have been explicitly separated into the term ε_ℓ, defined by equation (7). Thus, if any of the ε_ℓ are nonzero, then differential diffusion is present and the ε_ℓ provide a direct measure of its importance. Furthermore, comparing ε_ℓ with Υ^{exact} provides a quantitative measure of the rate at which differential diffusion affects the local concentration of element ℓ.

To evaluate the ε_ℓ defined in equation (7), the following must be specified:

1. Model for species diffusive fluxes, $\mathbf{j}_i$. In general, the diffusive flux of species i is given by the Stefan–Maxwell equations, and is a function of pressure, temperature, composition, and gradients in all species [1, 14–18] (see Appendix for more details).

2. Approximation for elemental diffusivities, D. For this study, these were obtained from $D = \lambda/(\mathrm{Le}\rho c_p)$ with $\mathrm{Le} = 1$, where λ is the mixture thermal conductivity, and c_p is the mixture isobaric heat capacity. In general, however, these diffusivities may be prescribed as functions of temperature, pressure, and composition, so long as all diffusivities are equal, i.e. $\mathrm{Le}_\ell = \mathrm{Le}_m$.

While the focus of this paper is on nonpremixed systems, the preceding analysis is equally applicable to premixed systems, and ε_ℓ defined by equations (6) and (7) may be evaluated in the same manner for both premixed and nonpremixed systems. The analysis based on the mixture fraction as presented in the next section, however, is more applicable to nonpremixed systems.

The N_e measures of DD, ε_ℓ, are complete. Other quantitative measures of DD may be obtained from a linear combination of the ε_ℓ. It may, however, be useful to have a single measure of DD rather than N_e independent measures. While there are many ways to arrive at a single measure, we choose one based on the mixture fraction.

2.1 *The mixture fraction*

The mixture fraction, f, may be written in terms of coupling functions, β, as [1]

$$f = \frac{\beta - \beta_0}{\beta_1 - \beta_0}, \tag{8}$$

where β_1 and β_0 are constants evaluated in the fuel and oxidizer streams, respectively. The coupling function, β, is defined in terms of the elemental mass fractions as

$$\beta = \sum_{\ell=1}^{N_e} \gamma_\ell Z_\ell = \sum_{\ell=1}^{N_e} \gamma_\ell \sum_{i=1}^{N_s} \frac{a_{\ell,i} W_\ell Y_i}{W_i}, \tag{9}$$

where γ_ℓ are weighting factors. The γ_ℓ are not unique, and several different values are commonly used [11, 12, 19], as shown in table 1. Given a choice of γ_ℓ, the composition of the pure streams (which determine β_0 and β_1), and the local composition, the local mixture fraction may be determined using equations (8) and (9). Note that by choosing Bilger's definition [19] for γ_ℓ, the stoichiometric mixture fraction (f_{st}) may be determined from equation (8) with $\beta = 0$. Unless explicitly stated otherwise, Bilger's choice of γ_ℓ will be used throughout this document.

2.1.1 Conservation equation for *f*. Combining equations (4), (8), and (9), a general evolution equation for the mixture fraction may be written as

$$\rho \frac{Df}{Dt} = \frac{-1}{\beta_1 - \beta_0} \sum_{\ell=1}^{N_e} \gamma_\ell \left(\sum_{i=1}^{N_s} \frac{a_{\ell i} W_\ell}{W_i} \nabla \cdot \mathbf{j}_i \right). \tag{10}$$

Table 1. Weighting factors (γ_ℓ) for various definitions of the mixture fraction.

	Bilger [19]	C	H	O
γ_C	$2/W_\mathrm{C}$	1	0	0
γ_H	$1/(2W_\mathrm{H})$	0	1	0
γ_O	$-1/W_\mathrm{O}$	0	0	1
γ_N	0	0	0	0

This equation makes no assumptions regarding the diffusive flux of each species, and is a completely general conservation equation for the mixture fraction as defined by equation (8). The species diffusive fluxes in equation (10) may be evaluated using different transport models including mixture averaged and full multicomponent transport with Soret effect. Equation (10), however, is not closed unless the species diffusive fluxes, $\mathbf{j}_i$, are given.

In the limiting case where species diffusive fluxes are given as $\mathbf{j}_i = -\rho D_i \nabla Y_i$ and all species diffusion coefficients are equal ($D_i = D$), it may be shown (using equations (3), (8), and (9)) that equation (10) reduces to

$$\rho \frac{Df}{Dt} = \nabla \cdot (\rho D \nabla f), \tag{11}$$

which is the conventional conservation equation for the mixture fraction [1–3]. In deriving equation (11), the fact that $\nabla \beta_0 = 0$ (since β_0 is a constant) was used. The only difference between equations (10) and (11) is the assumption of negligible DD. Thus, taking the difference between equations (10) and (11), a DD parameter, ε, may be defined as

$$\varepsilon \equiv \underbrace{\frac{-1}{\beta_1 - \beta_0} \sum_{\ell=1}^{N_e} \gamma_\ell \left(\sum_{i=1}^{N_s} \frac{a_{\ell i} W_\ell}{W_i} \nabla \cdot \mathbf{j}_i \right)}_{\Upsilon^{\text{exact}}} - \underbrace{\nabla \cdot (\rho D \nabla f)}_{\Upsilon^{\text{approx}}}. \tag{12}$$

The DD parameter, ε, may be interpreted in several ways:

1. ε provides a single, quantitative measure of DD for a given set of γ_ℓ. However, since the γ_ℓ are not unique, ε is not unique. As discussed previously, there are N_e independent measures of DD, ε_ℓ, given by equation (7). In fact, ε may be expressed as a simple linear combination of ε_ℓ as

$$\varepsilon = \frac{1}{\beta_1 - \beta_0} \sum_{\ell=1}^{N_e} \gamma_\ell \varepsilon_\ell, \tag{13}$$

   with analogous expressions relating Υ in equation (12) with Υ_ℓ in equation (7). Thus, ε may be interpreted as a *weighted average* measure of DD.
2. Many modelling approaches currently rely on the assumption that the mixture fraction is a conserved scalar, i.e. that its transport equation is given by equation (11). In this context, ε may also be interpreted as a source term that is neglected in equation (11), just as the ε_ℓ can be interpreted as source terms neglected in equation (5). The general evolution equation for the mixture fraction, equation (10), may thus be rewritten as

$$\rho \frac{Df}{Dt} = \nabla \cdot (\rho D \nabla f) + \varepsilon. \tag{14}$$

   Therefore, given a definition of the mixture fraction (i.e. a specific choice of γ_ℓ), the DD parameter, ε, provides a direct measure of the degree to which the mixture fraction is not conserved, and it is strictly caused by DD. In this context, ε may be interpreted as the local effect (in space and time) of DD on the evolution of the mixture fraction.

In the following discussion, we will use both of these interpretations of ε. To evaluate ε in general, the following must be specified:

(i) γ_ℓ to define the mixture fraction,
(ii) pure stream compositions to obtain β_0 and β_1,
(iii) expression for species mass diffusive fluxes, $\mathbf{j}_i$,
(iv) diffusivity, D, for the mixture fraction (typically from $D = \lambda/(\text{Le}\rho c_p)$ and specification of Le).

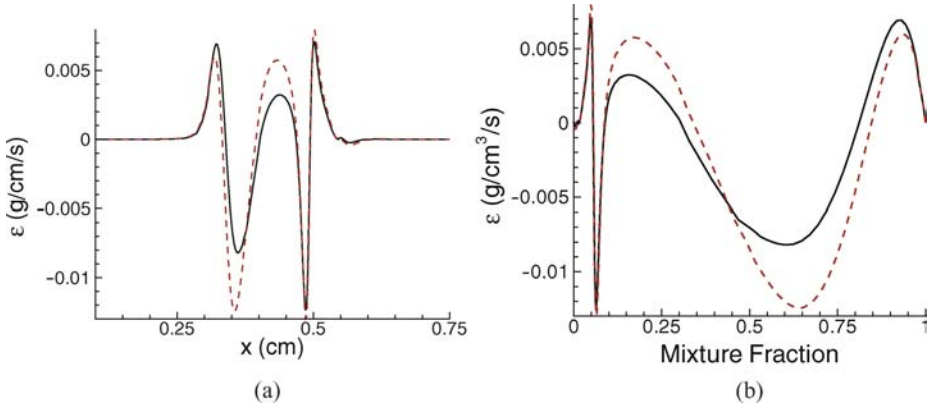

Figure 1. (a) ε as a function of position and (b) mixture fraction for mixture averaged (dashed line) and multicomponent (solid line) transport. In (a) fuel is at left and oxidizer is at right, with f_{st} located at $x \approx 0.5$. Fuel is CH_4 at 300 K, oxidizer is air at 300 K, strain rate of 300/s.

3. Results–laminar flames

In this section we consider the relative magnitude of Υ^{exact} and Υ^{approx} as defined by equation (12) for several one-dimensional, steady, opposed-flow diffusion flames.

First, a strained methane–air flame is considered. The fuel and oxidizer streams both have temperatures of 300 K, and are composed of pure methane and air respectively, for which $f_{st} = 0.0552$. The strain rate as defined in [20] is 300/s (the effect of strain rate on DD will be examined shortly). GRI 3.0 [21] was used for chemical kinetic, thermodynamic, and transport data. Mixture-averaged transport was used to determine the species diffusive fluxes (see the appendix for details). Figure 1 shows ε as a function of (a) position and (b) mixture fraction for one-dimensional laminar opposed-jet methane–air flames computed with mixture averaged (dashed line) and multicomponent (solid line) transport. On the rich side of the flame, multicomponent effects have a significant effect on DD. Near stoichiometric conditions, however, multicomponent and mixture-averaged transport appear to predict the same amount of DD. Although figure 1 shows that ε is moderately affected by differences between mixture-averaged and multicomponent transport for this flame, mixture-averaged transport will be used for species diffusive fluxes in all calculations presented in this work.

As mentioned in section 1, DD has historically been measured qualitatively by taking differences between various elemental mixture fractions [10–12]. Let $\zeta_{\ell m}$ represent the difference between elemental mixture fractions f_ℓ and f_m, where f_ℓ is obtained by setting $\gamma_{n\neq\ell} = 0$, $\gamma_\ell = 1$ (see table 1). Figure 2 shows several $\zeta_{\ell m}$ as well as the DD parameter, ε, as functions of f_{Bilger}. Note that attempting to quantify DD by $\zeta_{\ell m}$ leads to ambiguous results: it is not clear which $\zeta_{\ell m}$ (if any) is appropriate, and it is even less clear how large $\zeta_{\ell m}$ must be to be 'significant.' In other words, $\zeta_{\ell m}$ provides at best a qualitative indication of DD.

Let us now turn our attention to the DD parameters ε_ℓ and ε defined by equation (7) and (12), respectively. Figure 3(a) shows ε, Υ^{exact}, and Υ^{approx} as functions of f_{Bilger}. Comparing ε with Υ^{exact} provides a quantitative measure of DD. Note that there are several points near f_{st} where ε is around 50% of Υ^{exact}. In other words, the mixture fraction evolution given by equation (11) is incorrect by approximately 50% near f_{st}. This is shown quantitatively in figure 3(b), where $100 \times \varepsilon / \Upsilon^{\text{exact}}$ is shown as a function of f_{Bilger}. The relative amount of DD as shown in figure 3(b) can be interpreted as the percent error

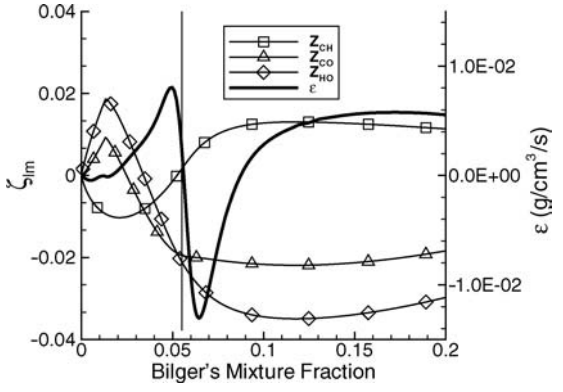

Figure 2. ε (right axis) and $\zeta_{\ell m}$ (left axis) as a function of f_{Bilger}. Fuel is CH_4 at 300 K, oxidizer is air at 300 K, strain rate of 300/s.

incurred in equation (11). It is a local and quantitative measure of the amount of DD occurring in a nonpremixed system with two feed streams. Note that the scaled DD measure, $\varepsilon/\Upsilon^{\text{exact}}$, becomes ill-defined as $\Upsilon^{\text{exact}} \to 0$, which happens near $f = 0.5$ for the methane–air flame.

The above discussion has focused on ε, which may be written as a linear combination of ε_ℓ as shown by equation (13). Given that the γ_ℓ are not unique (which implies that ε is not unique), it is useful to examine ε_ℓ, which form a complete basis for quantifying DD. Figure 4 shows ε_ℓ and ε using Bilger's choice for γ_ℓ. Bilger's mixture fraction does not incorporate dependence on Z_{N} since $\gamma_{\text{N}} = 0$ (see table 1). Thus, ε_{N} does not influence ε when Bilger's γ_ℓ are used. A notable result from figure 4, however, is that none of the ε_ℓ are zero. In other words, DD affects all of the elemental mass fractions. Thus, unless a choice of γ_ℓ could be found which made $\varepsilon = 0$, the effects of DD on the mixture fraction evolution cannot be eliminated and any scalar quantity derived from the elemental mass fractions will not be a conserved scalar as defined by equation (1). Figure 4(b) indicates that the scaled differential diffusion parameters, $\varepsilon_m/\Upsilon_m^{\text{exact}}$, for the elements are not well behaved near $f = 0$. This is due to $\Upsilon_m^{\text{exact}}$ crossing zero. For O, this occurs at $f \approx 0.015$ and for all elements, $\Upsilon_m^{\text{exact}} \to 0$ as $f \to 0$.

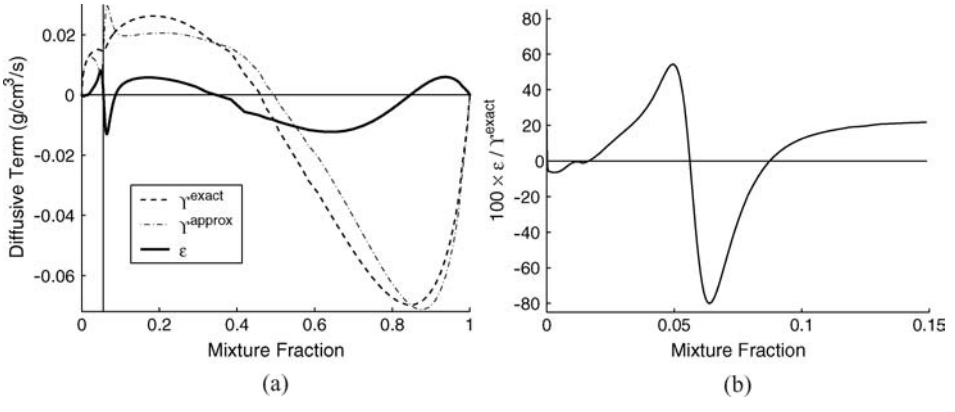

Figure 3. (a) shows Υ^{exact}, Υ^{approx}, and ε as functions of f_{Bilger}, with f_{st} indicated by the vertical line; (b) shows $100 \times \varepsilon/\Upsilon^{\text{exact}}$, versus f_{Bilger}. $f_{st} = 0.0552$.

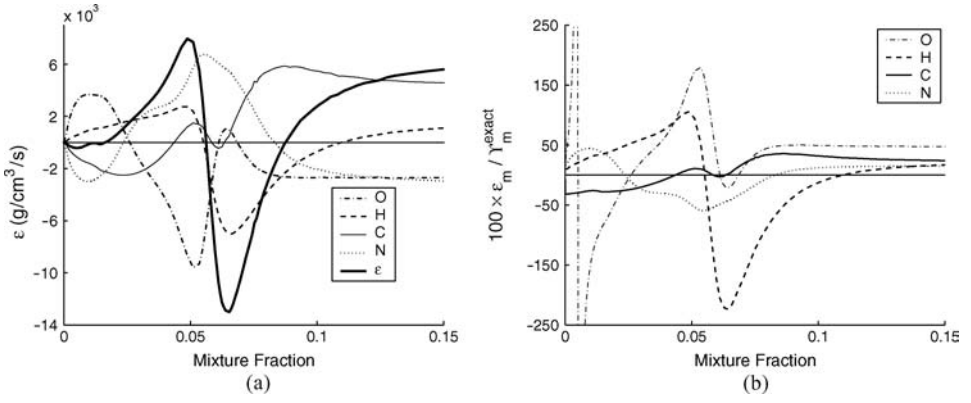

Figure 4. (a) shows elemental DD parameters, ε_ℓ, and $\varepsilon_{\text{Bilger}}$ (solid line) as functions of f_{Bilger}; (b) shows $100 \times \varepsilon_m / \Upsilon_m^{\text{exact}}$ versus f_{Bilger}. $f_{st} = 0.0552$.

3.1 *Effect of strain rate*

Previous studies of H_2–air opposed-jet flames have shown that DD measured by differences between elemental mixture fractions is relatively insensitive to the dissipation rate [12]. Nevertheless, there is also a trend showing decreased importance of DD with increasing dissipation rate [12]. Quantitative evaluation of the dependence of DD on strain rate provides some additional insight. Figure 5 shows $100 \times \varepsilon / \Upsilon^{\text{exact}}$ near f_{st} for various strain rates for two different flames. Figure 5(a) corresponds to a fuel composition of 90% H_2, 10% N_2 ($f_{st} = 0.0695$), and figure 5(b) corresponds to a fuel of pure methane ($f_{st} = 0.0552$). The fuel and oxidizer streams are both at 300 K, and the oxidizer is air (21% O_2, 79% N_2). The strain rates reported in figure 5 have units of s^{-1} and are based on the definition given in [20].

It is important to note that the results in figure 5 are scaled results, showing the *relative* importance of DD. Clearly, the *absolute* magnitude of ε increases with increasing strain rate, as the magnitude of all diffusion fluxes increase. Figure 5 is concerned with the relative importance of DD, i.e. the amount of the diffusive flux that is comprised of differential (as opposed to ordinary) diffusion.

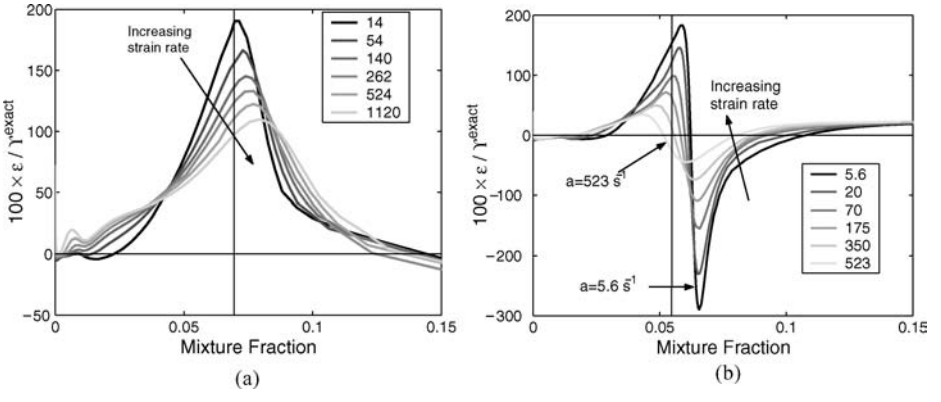

Figure 5. Scaled DD parameter, $\varepsilon / \Upsilon^{\text{exact}}$ for (a) H_2/N_2–air and (b) CH_4–air flames at various strain rates. Vertical line indicates f_{st}. Methane flames exhibit a much stronger dependence of DD on strain rate than hydrogen flames.

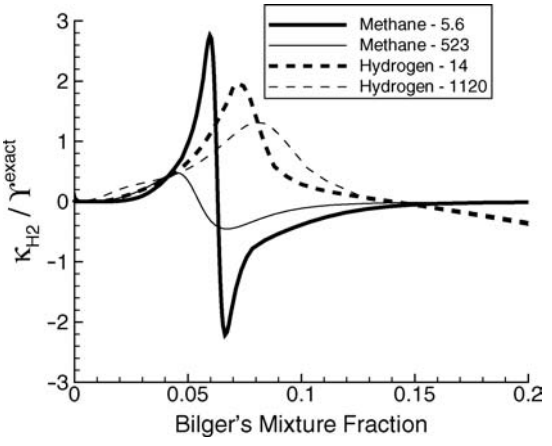

Figure 6. Scaled H_2 contribution to ε, (see equation (15)) for the methane flames (solid lines) and hydrogen flames (dashed lines) at low (thick lines) and high (thin lines) strain rates. κ_{H_2} is more sensitive to strain rate in the methane flame than the hydrogen flame. $f_{st} = 0.0552$.

Figure 5(b) shows that the methane flame exhibits a strong influence of strain rate on the relative amount of DD, particularly on the rich side of stoichiometric (near $f = 0.065$), where the relative contribution of DD varies from ∼300% to ∼50%. The hydrogen flame [figure 5(a)] shows a similar trend, but is not nearly as sensitive to the strain rate as the methane flame, varying from ∼200% to ∼100%. This is primarily caused by the generation of H_2 in the reaction zone of the methane flame. Since H_2 is a stable and highly diffusive intermediate, it strongly affects DD in the reaction zone of the methane flame. Furthermore, the diffusive fluxes of H_2 vary more strongly in the methane flame (where H_2 is both produced and consumed in the reaction zone) than in the hydrogen flame, where H_2 is a reactant and is only consumed in the reaction zone.

Figure 6 shows the contribution of H_2 to ε (denoted κ_{H_2}) for the hydrogen and methane flames at low and high strain rates, where

$$\kappa_i = \frac{-1}{\beta_1 - \beta_0} \sum_{\ell=1}^{N_e} \frac{\gamma_\ell W_\ell a_{\ell i}}{W_i} [\nabla \cdot \mathbf{j}_i + \nabla \cdot (\rho D \nabla Y_i)], \tag{15}$$

is the contribution to ε from species i, D is the mixture fraction diffusivity, and $\varepsilon = \sum_{i=1}^{N_s} \kappa_i$. H_2 provides the most significant contribution to ε for Bilger's mixture fraction. Figure 6 shows that κ_{H_2} for the methane flame is affected strongly by the strain rate, while κ_{H_2} for the hydrogen flame is weakly affected by the strain rate.

It is instructive to consider the relative importance of the κ_i as defined in equation (15). We have already shown that κ_{H_2} is important. Table 2 shows the L_1, L_2, and L_∞ norms for $\|\varepsilon - \varepsilon^*\|$, where ε^* is the partial sum of the species contributions to ε, $\varepsilon^* = \sum_{i=1}^{n} \kappa_i$. Bilger's choice of γ_ℓ is used. It is evident from table 2 that only a few species (of the 53 present in the chemical mechanism) make significant contributions to DD. Figure 7 shows $\kappa_{H_2}/\Upsilon^{exact}$, $\kappa_{CH_4}/\Upsilon^{exact}$, and $\varepsilon/\Upsilon^{exact}$ as functions of f_{Bilger} for the CH_4–air flame described in section 3. at a strain rate of 300/s. Figure 7 clearly shows that H_2 is a very significant contributor to DD near $f_{st} = 0.0552$, and the reactive fuel constituent (CH_4 in this case) is the most significant contributor in the rich region. The partial sum $\varepsilon^* = \kappa_{H_2} + \kappa_{CH_4}$ provides a fairly good approximation to ε over the entire range of mixture fraction space. The ordering shown in table 2 is independent of strain rate, and does not strongly depend on fuel composition (i.e. dilution by N_2 or the ratio between CH_4 and H_2). In fact, for H_2–air flames, the ordering

Table 2. Percent error norms for the truncated series $\varepsilon^* = \sum_{i=1}^{n} \kappa_i$. Results are for the CH_4–air flame described in section 3 at a strain rate of 300/s. For the H_2–air flames, the ordering remains the same, excluding the carbon-containing species.

n	$100 \times \|\varepsilon - \varepsilon^*\|_1$	$100 \times \|\varepsilon - \varepsilon^*\|_2$	$100 \times \|\varepsilon - \varepsilon^*\|_\infty$	Species
1	56	6.30	1.26	H_2
2	21	3.16	0.79	CH_4
3	13	1.74	0.39	H
4	7.3	0.81	0.15	C_2H_2
5	7.4	1.03	0.26	O_2
6	2.0	0.23	0.05	C_2H_4
7	4.7	0.68	0.17	CO

remains the same, excluding the carbon-containing species, and ε is represented fairly well by the contribution of H_2 alone. For example, for an opposed-jet flame with 90% H_2, 10% N_2 in the fuel at a strain rate of 314/s, approximating ε by κ_{H_2} alone gives an error of only 3% in the L_1 norm, $\|\varepsilon - \varepsilon^*\|_1$. Furthermore, in CO/$H_2$ flames (not shown here), H_2 and CO are the most significant contributors to DD (as both are constituents in the fuel). The DNS data from the turbulent jet flames described in the next section also support these conclusions. It should be noted, however, that the ordering is affected by the choice of γ_ℓ. The above results are for Bilger's choice of γ_ℓ.

Since H_2 and CH_4 are easily measured, ε may be approximated from experimental data, provided that the data are resolved highly enough that the appropriate terms in equation (12) can be computed.

4. Results—turbulent flames

In the context of LES of turbulent flows, the important question becomes: what is the importance of DD on the filter scale relative to the other terms in the filtered governing equations (e.g. the so-called turbulent diffusion term)? If DD is negligible on the filter scale, then all effects of DD may be relegated to a subgrid scale model and the mixture fraction may be treated as a conserved scalar on the filter scale, even if DD is occurring at the sub-filter scales.

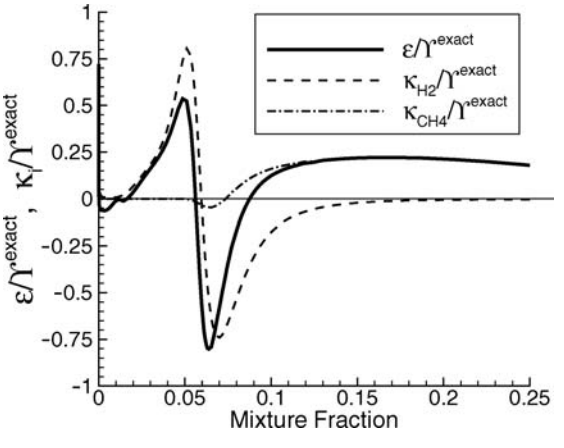

Figure 7. $\kappa_{H_2}/\Upsilon^{\text{exact}}$, $\kappa_{CH_4}/\Upsilon^{\text{exact}}$, and $\varepsilon/\Upsilon^{\text{exact}}$ as functions of f_{Bilger} for the CH_4–air flame described in section 3 at a strain rate of 300/s. $f_{st} = 0.0552$.

The general mixture fraction equation given by equation (16) can be rewritten in conservation form as

$$\frac{\partial(\rho f)}{\partial t} + \nabla \cdot (\rho \mathbf{u} f) = \underbrace{-\frac{1}{\beta_1 - \beta_0} \sum_{\ell=1}^{N_e} \gamma_\ell \sum_{i=1}^{N_s} \frac{a_{\ell i} W_\ell}{w_i} \nabla \cdot \mathbf{j}_i}_{\Upsilon^{\text{exact}}} . \tag{16}$$

Assuming commutivity between the filter and derivative operators, equation (16) may be spatially filtered to obtain

$$\frac{\partial(\bar{\rho}\tilde{f})}{\partial t} = -\nabla \cdot (\bar{\rho}\widetilde{\mathbf{u}f}) + \overline{\Upsilon^{\text{exact}}} \tag{17}$$

$$= -\nabla \cdot (\bar{\rho}\tilde{\mathbf{u}}\tilde{f}) + \overline{\Upsilon^{\text{exact}}} + \nabla \cdot \mathbf{Q}, \tag{18}$$

where $\tilde{\phi} = \phi - \phi''$ represents a Favre-filtered quantity, defined as $\tilde{\phi} = \overline{\rho\phi}/\bar{\rho}$, and $\mathbf{Q}$ is given as

$$\mathbf{Q} = \bar{\rho}(\tilde{\mathbf{u}}\tilde{f} - \widetilde{\mathbf{u}f}) = -\bar{\rho}\left[\underbrace{\widetilde{\mathbf{u}}\tilde{f} - \tilde{\mathbf{u}}\tilde{f}}_{\mathbf{Q}^L} + \underbrace{\widetilde{\mathbf{u}f''} + \widetilde{\mathbf{u}''}\tilde{f}}_{\mathbf{Q}^C} + \underbrace{\widetilde{\mathbf{u}''f''}}_{\mathbf{Q}^R}\right], \tag{19}$$

with $\mathbf{Q}^L$, $\mathbf{Q}^C$, and $\mathbf{Q}^R$ representing the Leonard, cross, and Reynolds terms, respectively. Equation (18) can be rewritten in terms of the DD parameter, ε, as

$$\frac{\partial(\bar{\rho}\tilde{f})}{\partial t} = \underbrace{-\nabla \cdot (\bar{\rho}\tilde{\mathbf{u}}\tilde{f})}_{1} + \underbrace{\nabla \cdot (\bar{\rho}D\widetilde{\nabla f})}_{2} + \underbrace{\nabla \cdot \mathbf{Q}}_{3} + \underbrace{\bar{\varepsilon}}_{4}, \tag{20}$$

which is an exact evolution equation for the filtered mixture fraction. Terms 1–4 are briefly described as

(i) convective transport on the filter scale;
(ii) diffusive transport on the filter scale, neglecting DD;
(iii) sub-filter scale turbulent transport (turbulent diffusion);
(iv) diffusive transport exclusively attributed to DD on the filter scale (a measure of DD on the filter scale).

Neglecting $\bar{\varepsilon}$ in equation (20) is equivalent to traditional expressions for the filtered mixture fraction transport equation. Clearly, the relative magnitude of the terms in equation (20) is a function of the filter width, Δ, since as $\Delta \to \Delta_{\text{DNS}}$, $\mathbf{Q} \to 0$.

4.1 *Description of the DNS cases*

DNS data from two-dimensional spatially evolving 'turbulent' jets have been analysed to determine the importance of DD. The DNS data sets were generated using Sandia's S3D code [22], which employs eighth-order explicit finite difference spatial treatment [23] and a fourth-order Runge–Kutta time integrator [24] to solve the compressible Navier–Stokes equations in fully conservative form. All thermodynamic and transport properties are taken to be functions of temperature, pressure, and composition.

The mean velocity, species mass fractions, and temperature are specified at the inlet boundary. Species compositions and temperature are found by first prescribing the mixture fraction profile. Given the mixture fraction profile on the inlet boundary, species and temperature profiles are specified using a flamelet solution. Velocity fluctuations are imposed in a time-dependent manner using pre-computed, spatially varying velocity fields adhering to the

von Karman–Pao kinetic energy spectrum [25]. These spatial velocity fluctuations are converted to temporal fluctuations using Taylor's hypothesis. This is reasonably accurate provided that the velocity fluctuations are small relative to the mean flow velocity, which is the case for the DNS cases considered herein. The transverse and outflow boundaries are nonreflecting with improvements to allow flames to exit the computational domain [26]. Additional details on the computational configuration are provided elsewhere [27].

Grid spacing was set to ensure adequate spatial resolution of the smallest structures in the flow field. For the DNS described herein, this corresponds to gradients of intermediate species through highly strained reaction zones.

Two DNS cases will be considered. The first case is a $CO/H_2/N_2$–air jet flame. The fuel stream is composed of (in mole%) 40% CO, 30% H_2, and 30% N_2, giving $f_{st} = 0.296$. Both fuel and oxidizer are both at 300 K, and the fuel stream (jet width) is approximately 5 mm. The mean fuel velocity at the inlet is about 60 m/s with an air co-flow of 10 m/s. The rms velocity fluctuations at the inlet are 300 cm/s, with an integral scale of 1 mm. The scalar dissipation rate at the inlet boundary is approximately 300/s. The domain size is 5×2 cm, with a grid spacing of approximately 45 μm. The kinetic mechanism employed for CO/H_2 oxidation includes 12 species and 33 reactions, and was developed by Yetter *et al.* [28, 29].

The second DNS case is a $CH_4/H_2/N_2$–air jet flame. The fuel stream contains (in mole%) 22.1% CH_4, 44.7% H_2, and 33.2% N_2 at 300 K and the oxidizer is air at 300 K ($f_{st} = 0.167$). The kinetic mechanism is a reduced mechanism based on GRI 3.0 which incorporates 17 species and 13 reactions [30]. The mean jet velocity is 52 m/s with a co-flow velocity of 10 m/s. Coherent velocity fluctuations with $|\boldsymbol{u}'| \approx 3.5$ m/s and a turbulence integral scale of 0.6 mm are superimposed on the velocity field in the fuel stream. The domain size is 6.6×2 cm, with a grid spacing of approximately 25 μm.

Figure 8 shows the dissipation rate, $\chi = 2D\nabla f \cdot \nabla f$, for the methane flame at 2.7 ms of simulation time (approximately two flow times), with the stoichiometric mixture fraction isocontour overlayed. Figure 8 shows that the DNS corresponds to the near-field of a spatially evolving jet, before the potential core collapses. All results presented herein should be considered with this in mind.

4.2 *DNS data analysis*

To assess the relative importance of DD on the filter scale, the DNS cases described previously were spatially filtered using a top hat filter kernel for filter widths Δ ranging from 1 to 32, where Δ refers to the filter width relative to the DNS grid spacing. At $\Delta = 1$, the conditional mean of ε on f and $\chi = 2D\nabla f \cdot \nabla f$ is qualitatively very similar to the results from one-dimensional flame studies such as those presented in figure 5.

We first consider the CO/H_2–air data. Figure 9 shows probability density functions (PDFs) for terms 1–4 in equation (20) normalized by $\partial(\bar{\rho}\tilde{f})/\partial t$, conditioned on being on the

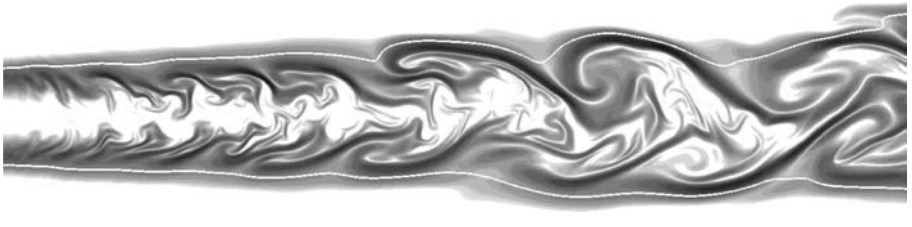

Figure 8. Dissipation rate field (logarithmic greyscale) with stoichiometric mixture fraction isocontour overlayed.

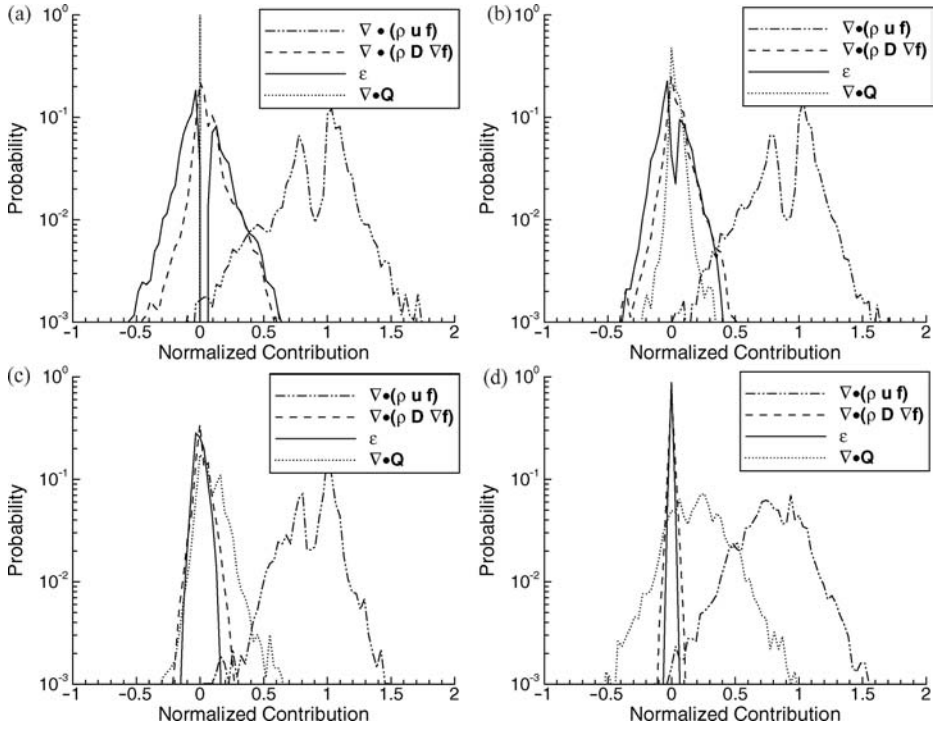

Figure 9. Normalized contributions to $\partial(\bar{\rho}\tilde{f})/\partial t$ corresponding to terms 1–4 in equation (20), for the CO/H_2–air DNS data. Results are conditioned on $f_{st} = 0.296$. (a) $\Delta = 1$; (b) $\Delta = 16$; (c) $\Delta = 32$; (d) $\Delta = 64$.

stoichiometric surface, $f_{st} = 0.296$. Results are shown for $\Delta = 1$ [figure 9(a)], $\Delta = 16$ [figure 9(b)], $\Delta = 32$ [figure 9(c)], and $\Delta = 64$ [figure 9(d)]. The terms indicated in each graph are spatially filtered and correspond to the terms in equation (20). Examining figure 9(a), it is apparent that the convective term, $\nabla \cdot (\bar{\rho}\tilde{\mathbf{u}}\tilde{f})$, is dominant. Comparing the approximate diffusive term, $\nabla \cdot (\bar{\rho}\widetilde{D\nabla f})$, with the DD term, ε, it is clear that the DNS exhibits a significant amount of DD at f_{st}. In fact, DD is larger than the approximate diffusive term on average. As expected, increasing Δ decreases the importance of molecular diffusion while increasing the importance of 'turbulent diffusion', $\nabla \cdot \mathbf{Q}$. Also of interest, however, is the observation that DD becomes less important relative to the approximate diffusive term as Δ increases, although this trend is not strong for the CH_4/H_2 data. Thus, in an LES where molecular diffusion is significant relative to turbulent diffusion, DD may also play a significant role on the filter-scale.

For the CO/H_2 data, the total filter-scale molecular diffusion, defined as $\overline{\Upsilon^{\text{exact}}} = \bar{\varepsilon} + \nabla \cdot (\bar{\rho}\widetilde{D\nabla f})$, is larger than the turbulent diffusion term, $\nabla \cdot \mathbf{Q}$, for $\Delta \lesssim 32$. At $\Delta = 64$, however, turbulent diffusion dominates over molecular diffusion.

We now turn our attention to the CH_4/H_2–air data. Figure 10 shows PDFs for terms 1–4 in equation (20) normalized by $\partial(\bar{\rho}\tilde{f})/\partial t$, and conditioned on being on the stoichiometric surface, $f_{st} = 0.167$. The first obvious difference between the CO/H_2 and CH_4/H_2 data sets is the relative importance of DD. For the CH_4/H_2 data, DD is very significant, and is substantially larger than the approximate diffusion term. The observation of DD being more significant in the turbulent CH_4/H_2 flames than the CO/H_2 flames is consistent with the results obtained in the laminar, one-dimensional opposed-jet calculations.

As Δ increases, the importance of $\bar{\varepsilon}$ relative to $\nabla \cdot (\bar{\rho}\widetilde{D\nabla f})$ decreases. This trend is much stronger in the CH_4/H_2 flame than in the CO/H_2 flame. This is likely owing to the generation

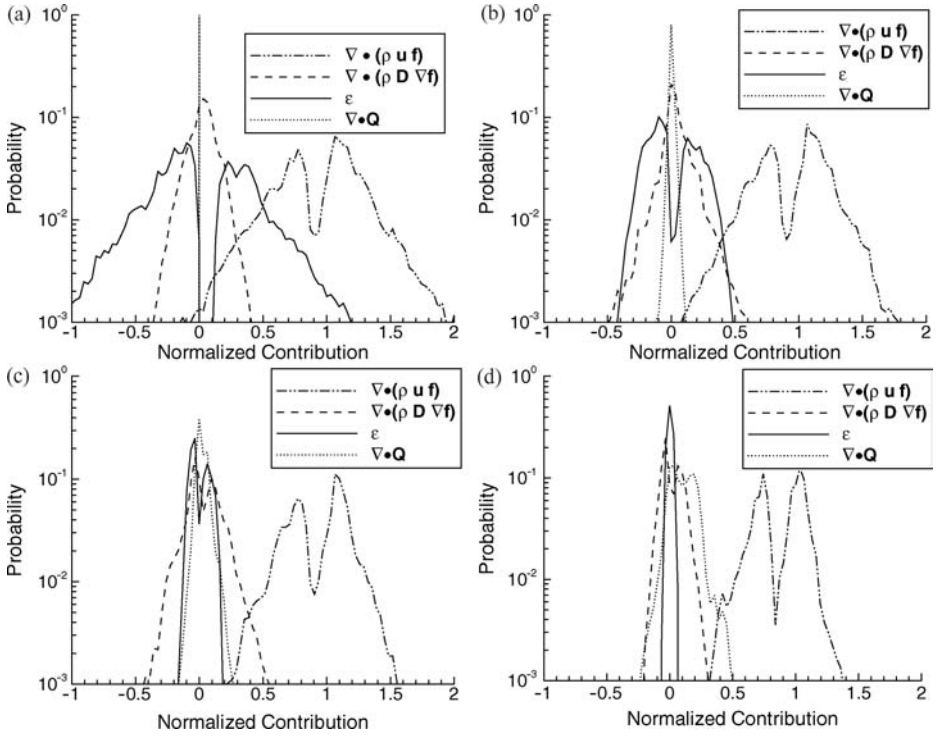

Figure 10. Normalized contributions to $\partial(\bar{\rho}\,\widetilde{f})/\partial t$ corresponding to terms 1–4 in equation (20), for the CH_4/H_2–air DNS data. Results are conditioned on $f_{st} = 0.167$. (a) $\Delta = 1$; (b) $\Delta = 16$; (c) $\Delta = 32$; (d) $\Delta = 64$.

of H_2 near f_{st} in the CH_2/H_2 flame (see the discussion surrounding figure 6). The H_2 generated in the flame zone is produced on a small scale and, therefore, it is more strongly attenuated by the filter.

The total molecular diffusion term, $\overline{\Upsilon^{\text{exact}}}$, remains significant even at $\Delta = 64$. Recall, however, that Δ is defined relative to the DNS grid spacing, and that the CH_4/H_2 flame requires significantly higher resolution for the intermediate species (25 μm versus 45 μm).

The results shown in figures 9 and 10 were conditioned on being on the stoichiometric surface. Results in the fuel stream indicate that DD is negligible at all filter widths, and show that filter-scale convection dominates over filter-scale molecular diffusion for all filter widths.

5. Conclusions

This paper has proposed a new method to quantify differential diffusion. In general, DD can be represented using N_e degrees of freedom, where N_e is the number of elements. By considering exact and 'conserved scalar' forms of the elemental conservation equations, N_e independent measures of DD were proposed. These are applicable in premixed or nonpremixed combustion. To obtain a single measure of DD particularly useful in nonpremixed combustion, the mixture fraction was introduced as a linear combination of the elemental mass fractions. A single measure of DD was, therefore, proposed as a particular linear combination of the N_e independent measures.

Results from one-dimensional laminar opposed-jet flame calculations demonstrate that DD near the stoichiometric mixture fraction can be sensitive to strain rate, particularly for

hydrocarbon flames. This sensitivity is attributed primarily to the generation of H_2 in the flame zone.

In terms of a single measure of DD based on Bilger's definition of the mixture fraction, H_2 is the most significant species contributor to DD near stoichiometric. This observation holds for flames containing CH_4, H_2, and CO in any proportions in the fuel stream, and is independent of strain rate. This implies that, if highly resolved spatial measurements of H_2 gradients can be made, experimental quantification of DD in the manner proposed herein is possible.

In the context of LES, data from direct numerical simulations of $CH_4/H_2/N_2$–air and $CO/H_2/N_2$–air flames were spatially filtered and analysed to determine the importance of DD relative to convection, and sub-filter terms in the filtered mixture fraction governing equation. As filter size increases, the importance of DD relative to 'approximate' molecular diffusion on the filter scale diminishes.

Appendix: Expressions for species diffusive fluxes

In the absence of thermal diffusion, the Maxwell–Stefan equations may be written as [1, 16–18, 31]

$$\mathbf{d}_i = -\sum_{j=1}^{N_s} \frac{X_i X_j(\mathbf{u}_i - \mathbf{u}_j)}{\mathcal{D}_{ij}} \tag{A.1}$$

where $\mathbf{u}_i$ is the velocity of species i, $\mathcal{D}_{ij}$ are the Maxwell–Stefan (binary) diffusion coefficients, X_i is the mole fraction of species i, and $\mathbf{d}_i$ is the diffusion driving force vector. The diffusion driving force for a mixture of ideal gases can be determined from irreversible thermodynamics as [16, 18]

$$\mathbf{d}_i = \nabla X_i + (X_i - Y_i)\nabla(\ln p) + \frac{\rho Y_i}{p}\left[\mathbf{f}_i - \sum_{j=1}^{N_s} Y_j \mathbf{f}_j\right] \tag{A.2}$$

where Y_i is the mass fraction of species i, and $\mathbf{f}_i$ is the body force on species i. In the case of gravity, $\mathbf{f}_i = \mathbf{f}_j = \mathbf{g}$ and the last term in equation (A.2) is identically zero.

Let us define the total mass flux of species i as $\mathbf{n}_i = \rho Y_i \mathbf{u}_i$, where $\mathbf{u}_i$ is the velocity of species i and ρ is the mass density. The species mass-diffusion flux relative to the mass-averaged system velocity, $\mathbf{j}_i$, is defined in terms of $\mathbf{n}_i$ as

$$\mathbf{n}_i = \mathbf{j}_i + \rho Y_i \mathbf{u} \tag{A.3}$$

where $\mathbf{u} = \sum_{i=1}^{N_s} Y_i \mathbf{u}_i$ is the mass-averaged system velocity. Using these definitions, equation (A.1) may be rewritten as

$$\mathbf{d}_i = -\sum_{j=1}^{N_s} \frac{X_i X_j(\mathbf{n}_i/Y_i - \mathbf{n}_j/Y_j)}{\rho \mathcal{D}_{ij}} \tag{A.4}$$

$$= -\frac{W}{\rho}\sum_{k=1}^{N_s} \frac{1}{\mathcal{D}_{ij}}\left(\frac{X_k}{W_i}\mathbf{j}_i - \frac{X_i}{W_k}\mathbf{j}_k\right) \tag{A.5}$$

where the relationships

$$Y_i W = X_i W_i, \tag{A.6}$$

$$W = \sum_{i=1}^{N_s} X_i W_i = \left(\sum_{i=1}^{N_s} Y_i/W_i\right)^{-1} \tag{A.7}$$

have been used. Equation (A.5) forms the basis for determining the diffusive fluxes in multicomponent computational fluid dynamics (CFD) since it relates the species mass diffusion fluxes relative to a mass-averaged velocity, $\mathbf{j}_i$, to the driving force, $\mathbf{d}_i$. Equation (A.5) is not, however, in a very convenient form. We would prefer to write the fluxes explicitly in terms of the diffusion driving force as (in matrix form)

$$(\mathbf{j}) = -\rho[D](\mathbf{d}) \tag{A.8}$$

where D_{ij} represent Fickian diffusion coefficients. Using the fact that the diffusive fluxes must sum to zero, we may write the flux of the nth species as $\mathbf{j}_n = -\sum_{k=1}^{N_s-1} \mathbf{j}_k$, and equation (A.5) may be rewritten as

$$\mathbf{d}_i = \frac{W}{\rho} \sum_{k=1}^{N_s-1} \left[\frac{-X_k}{W_i \mathcal{D}_{ik}} \mathbf{j}_i - \frac{1 - X_k}{W_i \mathcal{D}_{in}} \mathbf{j}_i + \frac{X_i}{W_k \mathcal{D}_{ik}} \mathbf{j}_k + \frac{X_i}{W_k \mathcal{D}_{in}} \mathbf{j}_k \right] \tag{A.9}$$

This equation may be written in matrix form for the system of $N_s - 1$ species as

$$(\mathbf{d}) = -\frac{W}{\rho}[B](\mathbf{j}) \tag{A.10}$$

where $[B]$ is a square matrix with dimensionality $(N_s - 1)$, whose elements are given as

$$B_{ik} = -X_i \left[\frac{1}{W_k \mathcal{D}_{ik}} - \frac{1}{W_n \mathcal{D}_{in}} \right] + \frac{\delta_{ik}}{W_i} \sum_{j=1}^{N_s-1} \left[\frac{X_j}{\mathcal{D}_{ij}} + \frac{1 - X_j}{\mathcal{D}_{in}} \right] \tag{A.11}$$

We may thus define

$$[D] \equiv W^{-1}[B]^{-1} \tag{A.12}$$

which is easily obtained given the composition, species molecular weights, and the binary diffusion coefficients, $\mathcal{D}_{ij}$. Note that $[D] = W^{-1}[B]^{-1}$ is a different definition of D_{ij} that is commonly used [16].

Alternative form

Occasionally it is more convenient to express diffusive flux driving force in terms of ∇Y_i rather than ∇X_i. This is easily accomplished by using the Jacobian J^{XY}. Thus, for the $N_s - 1$ species mass fractions, we have

$$(\nabla X) = [J^{XY}](\nabla Y) \tag{A.13}$$

$$(\nabla Y) = [J^{YX}](\nabla X) \tag{A.14}$$

with elements defined as

$$J_{ij}^{XY} = \frac{W}{W_i} \left[\delta_{ij} - W Y_i \left(\frac{1}{W_j} - \frac{1}{W_n} \right) \right] \tag{A.15}$$

and the inverse transformation $[J^{YX}] = [J^{XY}]^{-1}$ given by

$$J_{ij}^{YX} = \frac{W_i}{W} \left[\delta_{ij} - \frac{X_i}{W} (W_j - W_n) \right] \tag{A.16}$$

The matrices $[J^{XY}]$ and $[J^{YX}]$ have dimension $N_s - 1$.

If body forces act equally on all species ($\mathbf{f}_i = \mathbf{f}_j = \mathbf{f}$) and there are not significant pressure gradients ($\nabla \ln p \approx 0$), the diffusion driving force may be expressed as

$$(\mathbf{d}) = (\nabla X) = [J^{XY}](\nabla Y) \tag{A.17}$$

The resulting expression for the species diffusive fluxes can be written as

$$(\mathbf{j}) = \rho[D^{\circ}](\nabla Y) \tag{A.18}$$

where $[D^{\circ}] \equiv W^{-1}[B]^{-1}[J^{XY}]$

Binary reduction

In the case of a binary system, it is easily shown that $B_{11} = B = W/(W_1 W_2 \mathcal{D}_{12})$, and

$$\mathbf{j}_1 = -\rho \frac{Y_1 Y_2}{X_2 X_1} \mathcal{D}_{12} \mathbf{d}_1 \tag{A.19}$$

In the case in which $\mathbf{d}_i = \nabla X_i$, then equation (A.19) can be rewritten in terms of ∇Y_1 as

$$\mathbf{j}_1 = -\rho \mathcal{D}_{12} \nabla Y_1 \tag{A.20}$$

Simplified form: dilute mixtures

Consider a situation in which species n is in great abundance so that all other species are dilute. In the limit as $X_n \to 1$, equation (A.11) reduces to $B_{ii} = 1/(W_i \mathcal{D}_{in})$ and the species fluxes may be written as

$$\mathbf{j}_i = -\frac{\rho W_i}{W} \mathcal{D}_{in} \mathbf{d}_i = -\frac{\rho Y_i}{X_i} \mathcal{D}_{in} \mathbf{d}_i \tag{A.21}$$

In the absence of large pressure gradients ($\nabla \ln p \approx 0$) and external fields, which act unequally on species ($\mathbf{f}_i = \mathbf{f}_j = \mathbf{f}$), the driving force may be written as $\mathbf{d}_i = \nabla X_i$, and the species mass diffusive fluxes become

$$\mathbf{j}_i = -\frac{\rho Y_i}{X_i} \mathcal{D}_{in} \nabla X_i \tag{A.22}$$

Simplified form: mixture-averaged

Let us define the species diffusive fluxes as

$$\mathbf{j}_i = \rho D_i^{\text{mix}} \mathbf{d}_i \tag{A.23}$$

which may be written in terms of the total species fluxes, $\mathbf{n}_i$, as

$$\mathbf{j}_i = \mathbf{n}_i - Y_i \mathbf{n}_t \tag{A.24}$$

with $\mathbf{n}_i = \rho Y_i \mathbf{u}$. Substituting equation (A.4) for $\mathbf{d}_i$ and solving for D_i^{mix} gives

$$D_i^{\text{mix}} = (\mathbf{n}_i - Y_i \mathbf{n}_t) \left[\sum_{k \neq i}^{N_s} \frac{X_i X_k}{\mathcal{D}_{ik}} \left(\frac{\mathbf{n}_i}{Y_i} - \frac{\mathbf{n}_k}{Y_k} \right) \right]^{-1} \tag{A.25}$$

In the case of species i diffusing through $N_s - 1$ stagnant gases ($\mathbf{n}_{k \neq i} \to 0$, and $\mathbf{n}_i \to \mathbf{n}_t$), we obtain

$$D_i^{\text{mix}} = (1 - Y_i) \left[\frac{X_i}{Y_i} \sum_{k \neq i}^{N_s} \frac{X_k}{\mathcal{D}_{ik}} \right]^{-1} \tag{A.26}$$

Equation (A.26) is often derived using molar fluxes relative to molar-averaged velocities: $\mathbf{J}_i = \rho \mathsf{D}_i^{\text{mix}} \mathbf{d}_i / W$. In that case, $\mathsf{D}_i^{\text{mix}}$ is given as [18, 31]

$$\mathsf{D}_i^{\text{mix}} = (1 - X_i) \left[\sum_{k \neq i}^{N_s} \frac{X_k}{\mathcal{D}_{ik}} \right]^{-1} \tag{A.27}$$

While equation (A.26) is more appropriate for use in equation (A.23), at this level of approximation, differences between equations (A.26) and (A.27) may be insignificant.

A problem with the mixture-averaged approximation is that it does not necessarily satisfy the mass-conservation requirement of $\sum \mathbf{j}_i = 0$. Thus, a (constant) correction is sometimes added to equation (A.23) to ensure that the fluxes sum to zero [32–34],

$$\mathbf{j}_i = -\rho \frac{Y_i}{X_i} D_i^{\text{mix}} \nabla X_i + \mathbf{j}^{\text{corr}} \tag{A.28}$$

Acknowledgements

This work is supported by the Division of Chemical Sciences, Geosciences, and Biosciences, the Office of Basic Energy Sciences, the U S Department of Energy. We also gratefully acknowledge the Scalable Computing Research and Development department at Sandia National Laboratories, the National Energy Research Scientific Computing Center, and the Center for Computational Sciences at Oak Ridge National Laboratory, which provided computational resources for the calculations described herein.

References

[1] Williams, F. A., 1985, *Combustion Theory*, Second edition (Cambridge: Perseus Books).
[2] Dibble, R. W., Warnatz, J., and Maas, U., 1996, *Combustion*, First edition (Berlin: Springer).
[3] Peters, N., 2000, *Turbulent Combustion* (New York: Cambridge University Press).
[4] Lam, S. H. and Bellan, J., 2003, On de-coupling of Shvab-Zel'dovich variables in the presence of diffusion. *Combustion and Flame*, **132**, 691–696.
[5] Pitsch, H. and Peters, N., 1998, A consistent flamelet formulation for non-premixed combustion considering differential diffusion effects. *Combustion and Flame*, **114**, 26–40.
[6] Kronenburg, A. and Bilger, R. W., 1997, Modelling of differential diffusion effects in nonpremixed nonreacting turbulent flow. *Physics of Fluids*, **9**(5), 1435–1447.
[7] Nilsen, V. and Kosály, G., 1999, Differentially diffusing scalars in turbulence. *Physics of Fluids*, **9**(11), 3386–3397.
[8] Kronenburg, A. and Bilger, R. W., 2001, Modelling differential diffusion in nonpremixed reacting turbulent flow: Application to turbulent jet flames. *Combustion Science and Technology*, **199**, 175–193.
[9] Nilsen, V. and Kosály, G., 1999, Differential diffusion in turbulent reacting flows. *Combustion and Flame*, **117**, 493–513.
[10] Smith, L. L., Dibble, R. W., Talbot, L., Barlow, R. S., and Carter, C. D., 1995, Laser raman scattering measurements of differential molecular diffusion in turbulent nonpremixed jet flames of H_2/CO_2 fuel. *Combustion and Flame*, **100**, 153–160.
[11] Barlow, R. S., Fiechtner, G. J., Carter, C. D., and Chen, J. Y., 2000, Experiments on the scalar structure of turbulent $CO/H_2/N_2$ jet flames. *Combustion and Flame*, **120**, 549–569.
[12] Chen, Y. C. and Chen, J. Y., 1998, Fuel-dilution effect on differential molecular diffusion in laminar hydrogen diffusion flames. *Combustion Theory and Modelling*, **2**, 497–514.
[13] Hewson, J. C. and Kerstein, A. R., 2001, Stochastic simulation of transport and chemical kinetics in turbulent $CO/H_2/N_2$ flames. *Combustion Theory and Modelling*, **5**, 669–697.
[14] Maxwell, J. C., 1866, On the dynamical theory of gases. *Philosophical Transactions of the Royal Society*, **157**, 49–88.
[15] Stefan, J., 1871, Über das gleichgewicht und die Bewegung, insbesondere die Diffusion von Gasmengen. *Sitzungsberichte der K. Akademie der Wissenschaften in Wien*, **63**, 63–124.
[16] Hirschfelder, J. O., Curtis, C. F., and Bird, R. B., 1964, *The Molecular Theory of Liquids and Gases* (New York: Wiley).
[17] Giovangigli, V., 1999, *Multicomponent Flow Modeling* (Boston: Birkhauser).

[18] Taylor, R. and Krishna, R., 1993, *Multicomponent Mass Transfer* (New York: Wiley).
[19] Bilger, R. W., Stårner, S. H., and Kee, R. J., 1990, On reduced mechanisms for methane-air combustion in nonpremixed flames. *Combustion and Flame*, **80**(2), 135–149.
[20] Seshadri, K. and Williams, F. A., 1978, Laminar flow between parallel plates with injection of a reactant at high Reynolds number. *International Journal of Heat and Mass Transfer*, **21**(2), 251–253.
[21] Smith, G. P., Golden, D. M., Frenklach, M., Moriarty, N. W., Eiteneer, B., Goldenberg, M., Bowman, C. T., Hanson, R. K., Song, S., Gardiner Jr., W. C., Lissianski, V. V., and Qin, Z., URL http://www.me.berkeley.edu/gri_mech/.
[22] Mason, S. D. and Sutherland, J. C., 2002, *S3D: Sandia's Parallel F90 Direct Numerical Simulation Code for Turbulent Reacting Flows*. Sandia National Laboratories, Livermore, CA.
[23] Kennedy, C. A. and Carpenter, M. H., 1994, A comparison of several new numerical methods for the simulation of compressible shear layers. *Applied Numerical Mathematics*, **14**(4), 397–433.
[24] Kennedy, C. A., Carpenter, M. H., and Lewis, R. M., 2000, Low-storage, explicit Runge-Kutta schemes for the compressible Navier-Stokes equations. *Applied Numerical Mathematics*, **35**(3), 177–219.
[25] Hinze, J. O., 1975, *Turbulence*. Second edition (New York: MacGraw-Hill).
[26] Sutherland, J. C. and Kennedy, C. A., 2003, Improved boundary conditions for viscous, reacting, compressible flows. *Journal of Computational Physics*, **191**(2), 502–524.
[27] Sutherland, J. C., 2004, *Evaluation of Mixing and Reaction Models for Large-Eddy Simulation of Nonpremixed Combustion Using Direct Numerical Simulation*. PhD thesis, University of Utah, Salt Lake City, UT.
[28] Yetter, R. A., Dryer, F. L., and Rabitz, H., 1991, A comprehensive reaction mechanism for carbon-monoxide hydrogen oxygen kinetics. *Combustion Science and Technology*, **79**(1–3), 97–128.
[29] Mueller, M. A., Kim, T. J., Yetter, R. A., and Dreyer, F. L., 1999, Flow reactor studies and kinetic modeling of the H_2/O_2 reaction. *International Journal of Chemical Kinetics*, **31**(2), 113–125.
[30] Barlow, R. S., Karpetis, A. N., Frank, J. H., and Chen, J. Y., 2001, Scalar profiles and NO formation in laminar opposed-flow partially premixed methane/air flames. *Combustion and Flame*, **127**, 2102–2118.
[31] Bird, R. B., Stewart, W. E., and Lightfoot, E. N., 1960, *Transport Phenomena* (New York: Wiley).
[32] Coffee, T. P. and Heimerl, J. M., 1981, Transport algorithms for premixed, laminar steady-state flames. *Combustion and Flame*, **43**, 273–289.
[33] Ramshaw, J. D., 1990, Self-consistent effective binary diffusion in multicomponent mixtures. *Journal of Non-Equilibrium Thermodynamics*, **15**, 295.
[34] Ramshaw, J. D. and Chang, C. H., 1996, Friction-weighted self-consistent effective binary diffusion approximation. *Journal of Non-Equilibrium Thermodynamics*, **21**, 223–232.